

# Surface-Enhanced Raman Scattering of 4-Nitrothioanisole in Ag Sol

Kwan Kim,\* Seung Joon Lee, and Kyung Lock Kim

Laboratory of Intelligent Interfaces, School of Chemistry and Molecular Engineering,  
Seoul National University, Seoul 151-742, Korea

Received: June 3, 2004; In Final Form: August 7, 2004

Surface-enhanced Raman scattering (SERS) of 4-nitrothioanisole (4-NTA) is investigated in Ag sol. The molecule is found to adsorb on Ag as 4-NTA via the sulfur atom. Upon irradiation by an argon ion laser at 514.5 nm, the molecule is, however, subjected to two consecutive surface-induced photoreactions, namely C–S bond scission followed by nitro to amine conversion. Accordingly, the SERS spectrum of 4-NTA becomes the same as that of 4-aminobenzenethiolate adsorbed on Ag. Electrochemical analyses of 4-NTA at the Ag electrode combined with SERS measurements in concentrated sodium borohydride also suggest that the C–S bond scission takes place prior to the nitro to amine conversion.

## 1. Introduction

Since the discovery of surface-enhanced Raman scattering (SERS), there have been many theoretical and experimental studies on this effect.<sup>1–4</sup> Although the exact mechanism of SERS is still a matter of some controversy, it is generally accepted that two enhancement mechanisms, one a long range electromagnetic (EM) effect and the other a short range chemical (CHEM) effect, are simultaneously operative. The EM mechanism is based on the amplified electromagnetic field generated upon optical excitation of surface plasmon resonance of nanoscale surface roughness features in the 10–100 nm range,<sup>5–9</sup> while the CHEM enhancement mechanism is associated with the electronic coupling of molecules adsorbed on certain surface sites in atomic-scale roughness (such as atomic clusters, terraces, and steps) with the surface, leading to a situation similar to resonance Raman scattering.<sup>10–12</sup> Both mechanisms suggest the possibility of enhanced absorption and enhanced photochemistry for surface-adsorbed molecules.<sup>13–16</sup> Direct observation of a surface-enhanced photochemical reaction has indeed been reported. For example, photoreduction of methyl viologen,<sup>17</sup> as well as photodecomposition of azo compounds,<sup>18</sup> was confirmed to occur on silver. Aromatic acid has been reported to readily photodegrade on aggregated Ag nanocrystals.<sup>19</sup> Moreover, Suh and co-workers<sup>20–25</sup> invented the capillary flow method to quantitate by SERS the photochemical kinetics of various molecules adsorbed on colloidal silver surfaces and had successfully examined the photoreaction of phthalazine, the photodesorption of diiodobenzene and 4-vinylbenzoic acid, and the photoisomerization of maleic acid.

In our earlier SERS study, aromatic sulfides adsorbed on the surfaces of colloidal silver sol were found to undergo surface reactions involving facile cleavage of C–S bonds by 514.5 nm radiation;<sup>26–30</sup> such a reaction was found to hardly occur for the alkyl sulfides such as dimethyl sulfide and diethyl sulfide adsorbed on the colloidal silver surface.<sup>31</sup> Methyl phenyl sulfide (MPS), as well as benzyl phenyl sulfide (BPS), is exclusively decomposed into benzenethiolate on the silver surface, while dibenzyl sulfide (DBS) and benzyl methyl sulfide (BMS) are

converted into benzyl mercaptide by the 514.5 nm radiation. These molecules do not undergo such reactions on a gold surface, however.<sup>29,32</sup>

Several SERS studies have suggested that nitro molecules are also subjected to photoreaction on the silver surface.<sup>33</sup> The SERS spectral features of 4-nitrobenzenethiol (4-NBT)<sup>34–36</sup> and 4-nitrobenzoic acid (4-NBA)<sup>37</sup> on silver were recently found to be coincident with those of 4-aminobenzenethiol (4-ABT) and 4-aminobenzoic acid (4-ABA) on Ag, respectively. Much the same conclusion was derived not only from the X-ray photoelectron spectroscopy measurement but also from a coupling reaction conducted to form amide bonds.<sup>34</sup> The surface-induced photoreaction thereby allowed us to prepare patterned binary monolayers on Ag that showed different chemical reactivities.<sup>29,34</sup> Using the binary monolayers as a lithographic template, we could also conduct site selective chemical reactions.<sup>34</sup>

In conjunction with the above implications, we report herein the adsorption and photoreaction characteristics of 4-nitrothioanisole (4-NTA) on Ag revealed by SERS. The first concern in this work is whether C–S bond scission will occur for 4-NTA adsorbed on Ag by the irradiation of an Ar<sup>+</sup> laser at 514.5 nm. The second concern is to determine whether the nitro group in 4-NTA will also be converted to amine. The species responsible for the SERS spectrum of 4-NTA in Ag sol would be 4-NTA itself and/or 4-(methylthio)aniline, 4-NBT, 4-ABT, and methyl mercaptide. Both the C–S bond scission and the nitro to amine conversion are reductive reactions that require the electron transfer from Ag to 4-NTA. In this respect, the present study is expected to provide valuable information in connection with the usefulness of Ag nanoparticles acting as moderate photoelectron emitters.

## 2. Experimental Section

The method of preparation of aqueous Ag sol has been reported previously. Briefly, approximately 10 mL of 10<sup>−3</sup> M AgNO<sub>3</sub> solution was added dropwise to 30 mL of 2 × 10<sup>−3</sup> M NaBH<sub>4</sub> solution, which was chilled to ice temperature. The resulting Ag sol solution was stable for several weeks. An ethanol solution of 4-nitrothioanisole (Aldrich Chemical Co., 4-NTA) was added to the Ag sol to give a final adsorbate

\* To whom all correspondence should be addressed: Phone +82-2-8806651; fax +82-2-8891568; e-mail kwankim@plaza.snu.ac.kr.

concentration of  $\sim 10^{-4}$  M. When the aggregation of silver sol particles did not occur easily, a small amount of  $\text{BaCl}_2$  was added to induce the aggregation. After the sol solution changed from yellow to bluish green, poly(vinylpyrrolidone) (PVP, MW = 360 000) was added as a stabilizer whose concentration was  $\sim 0.01\%$  in the final solution. The chemicals otherwise specified were reagent grade, and triply distilled water, of resistivity greater than  $18.0 \text{ M}\Omega\cdot\text{cm}$ , was used in making aqueous solutions.

Raman spectra were obtained by using a Renishaw Raman system Model 2000 spectrometer equipped with an integral microscope (Olympus BH2-UMA). The 514.5 nm radiation from a 20 mW air-cooled argon ion laser (Melles-Griot Model 351MA520) was used as the excitation source. Raman scattering was detected with  $180^\circ$  geometry with a Peltier cooled ( $-70^\circ\text{C}$ ) charge coupled device (CCD) camera ( $400 \times 600$  pixels). A glass capillary (KIMAX-51) with an outer diameter of 1.3–1.5 mm was used as a sampling device. To minimize the laser-induced changes in the SERS spectra, sample solutions were sometimes made to flow through the glass capillary using a syringe pump (Sage Instrument Model 341) with a variable flow rate. The data acquisition time was usually 90 s. The holographic grating (1800 grooves/mm) and the slit allowed the spectral resolution to be  $1 \text{ cm}^{-1}$ . The Raman band of a silicon wafer at  $520 \text{ cm}^{-1}$  was used to calibrate the spectrometer, and the accuracy of the spectral measurement was estimated to be better than  $1 \text{ cm}^{-1}$ . The Raman spectrometer was interfaced with an IBM PC, and the spectral data were analyzed with Renishaw WiRE software v.1.2 based on the GRAMS/32C suite program (Galactic Industries).

To help interpret the SERS spectral features of 4-NTA in Ag sol, SERS spectra, as well as normal Raman (NR) spectra of 4-(methylthio)aniline (4-MTA), 4-nitrobenzenethiol (4-NBT), 4-aminobenzenethiol (4-ABT), and methyl mercaptide, were also obtained. In addition, a cyclic voltammetric study was conducted for 4-NTA and 4-MTA. The electrochemical cell consisted of three electrodes, that is, an Ag working electrode, a Pt counter electrode, and a saturated calomel reference electrode (SCE), and the electrode potential was controlled using a CH Instrument Model 600 Electrochemical system.

### 3. Results and Discussion

The SERS spectra of 4-nitrobenzenethiol (4-NBT) and 4-aminobenzenethiol (4-ABT) in silver sol are shown in parts a and b, respectively, of Figure 1, which have been obtained to aid in the interpretation of the SERS spectrum of 4-nitrothioanisole (4-NTA). To minimize laser-induced changes in the SERS spectra, the sample solutions were made to flow through the glass capillaries using a syringe pump with a constant flow rate. In fact, all the peaks in Figure 1a and b can be attributed to 4-nitrobenzenethiolate and 4-aminobenzenethiolate, respectively. The complete absence of the S–H stretching peak in the SERS spectra, observable at  $2548$  and  $2550 \text{ cm}^{-1}$ , respectively, for pure 4-NBT and 4-ABT indicates that 4-NBT, as well as 4-ABT, is adsorbed on Ag as thiolate after the S–H bond cleavage. The prominent SERS peak at  $1336 \text{ cm}^{-1}$  in Figure 1a can be assigned to the symmetric stretching vibration of the nitro group ( $\nu_s(\text{NO}_2)$ ). This indicates that the nitro group is not subjected to change solely due to the surface adsorption of 4-NBT on Ag. However, 4-NBT on Ag can be subjected to surface-induced photoreaction by the irradiation of an argon ion laser at 514.5 nm. This is evident from the SERS spectrum of 4-NBT obtained in the static condition. Its SERS spectral feature (see Figure 1c) is obviously different from that obtained under

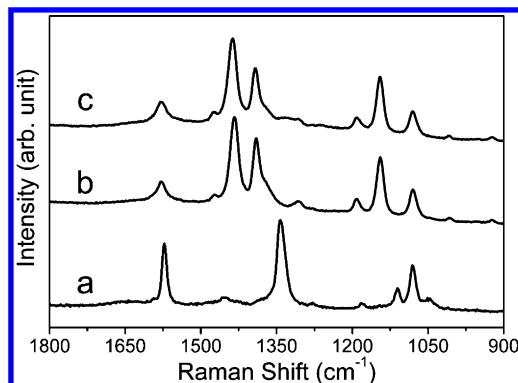


**Figure 1.** SERS spectra of (a) 4-nitrobenzenethiol (4-NBT) and (b) 4-aminobenzenethiol (4-ABT) in silver sol, taken while flowing the sample solutions through a glass capillary to minimize photoinduced reaction. (c) SERS spectrum of 4-NBT in silver sol taken in static condition.

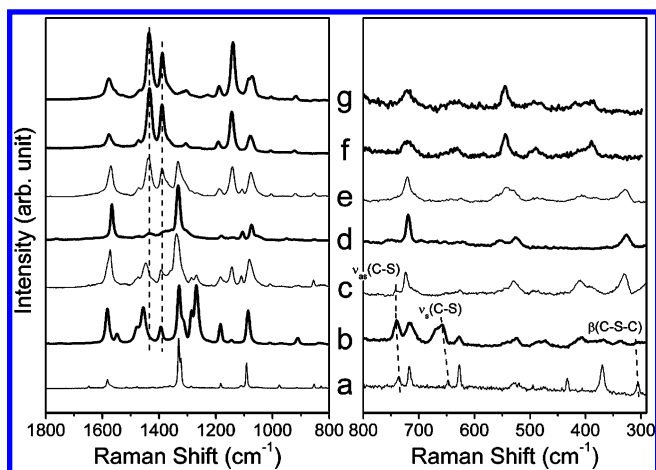


**Figure 2.** (a) Normal Raman (NR) spectrum of neat 4-nitrothioanisole (4-NTA) and its SERS spectra in silver sol, taken while flowing the sample solutions through a glass capillary at the flow rate of (b) 0.06, (c) 0.03, (d) 0.02, and (e)  $0.0032 \text{ mL}\cdot\text{s}^{-1}$ . SERS spectra of (f) 4-NTA and (g) 4-(methylthio)aniline (4-MTA) in silver sols in static condition. The dashed lines are drawn only as a guide to the eye, and the arrows in (a), (b), and (c) denote the spectral signatures of sulfide (see text).

the fluid condition (see Figure 1a). Instead, the spectral pattern in Figure 1c is comparable to that of 4-ABT in Figure 1b. The SERS spectral pattern of 4-ABT itself is independent of the measuring condition; that is, the spectrum obtained in the static condition differs little from that taken under the fluid condition. The present observation clearly supports the previous contention that 4-NBT adsorbed on Ag is converted in ambient conditions to 4-ABT upon irradiation by an argon ion laser (514.5 nm).

In Figure 2a and b are shown the normal Raman (NR) spectrum of neat 4-NTA and its SERS spectrum in silver sol, both of which were obtained with samples flowed through glass capillaries using a syringe pump. The two spectra exhibit a decent correlation with each other. Although a few peaks related to the vibrational modes involving sulfur are more or less shifted, the bands due to the benzene ring modes appear nearly at the same position in the two spectra. The  $\nu_s(\text{NO}_2)$  band is also clearly identified in both spectra. This suggests that the species responsible for Figure 2b is the adsorbed 4-NTA. Specifically, the bands due to the CSC bending, CS symmetric stretching, and CS asymmetric stretching vibrations appear at 310, 658, and  $741 \text{ cm}^{-1}$ , respectively, in Figure 2b while their counterparts are observed at 305, 648, and  $736 \text{ cm}^{-1}$ , respectively, in Figure 2a. The appearance of both the CSC bending and the CS

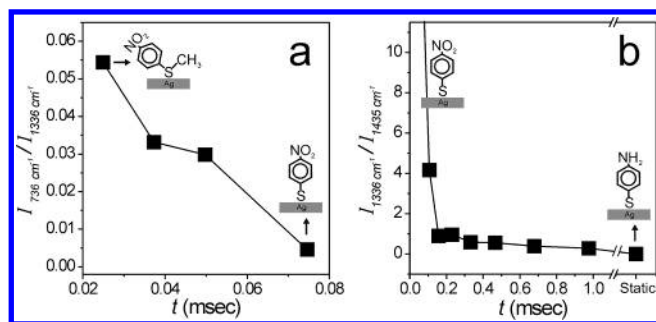


**Figure 3.** (a) Relative intensities of two representative SERS peaks of 4-NTA and 4-NBT, that is,  $I(736 \text{ cm}^{-1}, \nu_{\text{as}}(\text{C}-\text{S}))/I(1336 \text{ cm}^{-1}, \nu_{\text{s}}(\text{NO}_2))$ , drawn versus the laser exposure time. (b) Relative intensities of two representative SERS peaks of 4-NBT and 4-ABT, that is,  $I(1336 \text{ cm}^{-1}, \nu_{\text{s}}(\text{NO}_2))/I(1435 \text{ cm}^{-1}, \nu(\phi-\text{NH}_2))$ , drawn versus the laser exposure time. In the insets are depicted the products formed in the consecutive surface-induced photoreaction of 4-NTA on Ag.

symmetric stretching bands in the SERS spectrum suggests that C–S bond scission is not in fact feasible on the silver surface, as concluded for other sulfides in earlier SERS studies.<sup>26–30</sup> In addition, the fact that the bands due to modes involving sulfur are exclusively shifted indicates that 4-NTA is attached to the silver surface via its sulfur atom.

We have recorded another SERS spectrum for 4-NTA in Ag sol. The SERS spectrum shown in Figure 2f was taken with the sample kept in a sealed glass capillary, using the 514.5 nm excitation wavelength. Its general pattern looks quite different from that in Figure 2b. It is to be noted, however, that the SERS spectrum of 4-NTA in Figure 2f is remarkably similar to that of 4-ABT in Figure 1b. The band positions, as well as the relative band intensities, are almost the same for the two spectra. The species responsible for Figure 2f can thus be assumed to be 4-aminobenzenethiolate. This implies that not only  $\text{H}_3\text{C}-\text{S}$  bond scission but also nitro to amine conversion take place for 4-NTA on Ag upon irradiation by an argon ion laser at 514.5 nm. Consulting data from the literature,<sup>34–36</sup> the present observation is not unreasonable.

To assess the relative ease of the C–S bond scission and the nitro to amine conversion, we have subsequently recorded a series of SERS spectra for 4-NTA in Ag sol as a function of laser exposure time; the laser exposure time was controlled by changing the flow rate of the sample solution.<sup>38</sup> The SERS spectra in Figure 2b–e were obtained consecutively by decreasing the flow rate, thus representing spectra obtained in order of increasing laser exposure time. It is evident from Figure 2b–e that the SERS spectral features of 4-NTA are very dependent on the laser exposure time. In fact, the spectral pattern in Figure 2d is surprisingly in accord with that in Figure 1a, indicating that only the C–S bond scission can take place for 4-NTA to produce 4-NBT on Ag. Increasing further the laser exposure time, the spectral pattern gradually bears a resemblance to that of 4-ABT on Ag, as can be seen in Figure 2e. Finally, in static conditions the SERS spectral features of 4-NTA become exactly the same as those of 4-ABT on Ag, as already mentioned (see Figure 2f). For reference, we confirmed separately that the SERS spectrum of 4-(methylthio)aniline (4-MTA) in Ag sol shown in Figure 2g is much the same as that of 4-NTA in Figure 2f. All of these observations suggest that C–S bond scission must proceed prior to nitro to amine conversion when 4-NTA on Ag is exposed to an argon ion laser at 514.5 nm.

In Figure 3a are shown the relative intensities of two representative SERS peaks of 4-NTA and 4-NBT, that is, the peak at  $736 \text{ cm}^{-1}(\nu_{\text{as}}(\text{C}-\text{S}))$  and that at  $1336 \text{ cm}^{-1}(\nu_{\text{s}}(\text{NO}_2))$ , drawn versus the laser exposure time. Herein, a value of “zero”

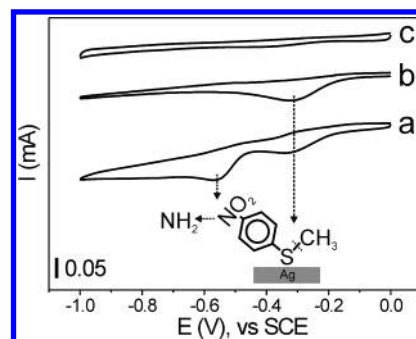


**Figure 4.** Cyclic voltammograms of 1 mM solutions of (a) 4-NTA and (b) 4-MTA, and (c) their supporting electrolyte, 0.1 M  $\text{Na}_2\text{SO}_4$ , in a 1:1 volume mixture of  $\text{H}_2\text{O}$  and  $\text{CH}_3\text{OH}$ , on an Ag electrode at a 20 mV/s scan rate. In the inset are depicted the specific chemical sites involved in the electrochemical reduction of 4-NTA on Ag.

corresponds to a complete conversion of 4-NTA to 4-NBT on Ag. The sulfide to thiolate conversion is seen to occur within 0.075 ms under the laser illumination. In a similar manner, the feasibility of the nitro to amine conversion was examined, referring to the relative intensities of two representative SERS peaks of 4-NBT and 4-ABT, that is, the peak at  $1336 \text{ cm}^{-1}(\nu_{\text{s}}(\text{NO}_2))$  and that at  $1435 \text{ cm}^{-1}(\nu(\phi-\text{NH}_2))$ . As can be seen in Figure 3b, the nitro to amine conversion also occurs very rapidly, but comparing the two kinetic plots in Figure 3, the C–S bond scission must proceed prior to the nitro to amine conversion, as presumed previously, when 4-NTA on Ag is exposed to an argon ion laser at 514.5 nm.

To obtain further information on the relative ease of the sulfide to thiolate and nitro to amine conversions, a cyclic voltammetric study is conducted for 4-NTA and 4-MTA at Ag electrodes. The cyclic voltammograms (CVs) obtained for 4-NTA and 4-MTA are shown in parts a and b, respectively, of Figure 4; the concentrations of sulfides were  $1.0 \times 10^{-3} \text{ M}$  for both cases. For comparison, the CV of the supporting electrolyte, 0.1 M  $\text{Na}_2\text{SO}_4$  in a 1:1 volume mixture of  $\text{H}_2\text{O}$  and  $\text{CH}_3\text{OH}$ , is shown in Figure 4c. The voltammetric feature in Figure 4c indicates that the electrolyte itself does not experience any significant electrochemical reaction in the potential region of  $-1.0$  to  $\sim 0 \text{ V}$  vs SCE. In sulfide solutions, only cathodic peaks are observed, indicating that the product formed in the initial reduction is not reoxidized at any rate. The CVs show that the electrochemical reduction begins at  $-0.20 \text{ V}$  vs SCE for both sulfides investigated, that is, 4-NTA and 4-MTA. In addition, the electrochemical reduction of both sulfides persists until the electrode potential reaches  $-0.80 \text{ V}$  vs SCE. Nonetheless, there are clear differences between the CVs of 4-NTA and 4-MTA. The cathodic current in Figure 4a is obviously larger than that in Figure 4b. It is also informative to note that two separate cathodic peaks appear at  $-0.3$  and  $-0.55 \text{ V}$  vs SCE in Figure 4a while only one peak appears at  $-0.3 \text{ V}$  vs SCE in Figure 4b. These differences must be attributed to the occurrence of two separate reductive reactions in the CV of 4-NTA. In the inset in Figure 4 are depicted the specific chemical sites involved in the electrochemical reduction of 4-NTA on Ag.

In fact, the cyclic voltammetric features of 4-MTA differ little from those of other sulfides such as benzyl phenyl sulfide (BPS) and dibenzyl sulfide (DBS).<sup>28</sup> The reduction of BPS to benzenethiolate, for instance, commences at  $-0.20 \text{ V}$  and continues up to  $-0.80 \text{ V}$  vs SCE; once reduced, no electrochemical reaction takes place in the potential range between  $-0.9$  and  $0.1 \text{ V}$  vs SCE. It is also informative to recall the fact that the reduction of 4-NBT to 4-ABT begins at  $-0.30 \text{ V}$  and is completed at  $-0.70 \text{ V}$  vs SCE.<sup>39</sup> The oxidation of 4-ABT is



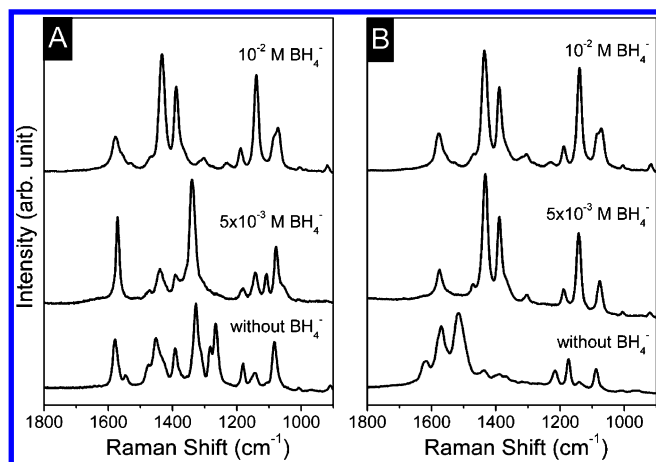


**Figure 5.** SERS spectra of (A) 4-NTA and (B) 4-MTA in silver sols containing different amounts of excess  $\text{NaBH}_4$ , taken while flowing the sample solutions through a glass capillary to minimize photoinduced reaction.

found, on the other hand, not to take place below 0.1 V vs SCE. These data are all in conformity with the cyclic voltammetric differences between 4-NTA and 4-MTA. Energetically, the electrochemical transformation seems thus to be in conformity with the photolysis of 4-NTA on Ag by an argon ion laser at 514.5 nm.

In an earlier investigation, the SERS spectrum of BPS was observed to change depending on the concentration of borohydride ion in the Ag sol solution.<sup>27</sup> Even under conditions where surface photoreaction was not likely to occur, BPS decomposed, yielding the SERS spectrum of adsorbed benzenethiolate, when an excess  $\text{NaBH}_4$  was present in the sol solution. This was attributed to the lowering of the surface potential by  $\text{BH}_4^-$ , and its validity was proven in a later study demonstrating the electrochemical reduction of organic sulfides to thiolates by means of SERS and cyclic voltammetry.<sup>28</sup> One intriguing observation was that the effective sol surface potential measured by a silver wire electrode dipped in the sol solution was 0.3 V larger than the actual potential. Such a discrepancy may be associated with the catalytic property of colloidal Ag particles. Pal et al.<sup>40</sup> demonstrated in recent years using UV/vis absorption spectroscopy that silver nanoparticles are very efficient catalysts for facilitating the reduction of various organic molecules by borohydride.<sup>40</sup> The catalytic efficiency of Ag nanoparticles for electron transfer was explained by their size dependent redox properties, which regulated their role as an electron relay system. The required potential of the nanoparticles was claimed to lie between the thresholds of the potentials of the donor (e.g., more negative,  $\text{BH}_4^-$ ) and the acceptor (e.g., more positive, organic compounds). On these grounds, the effect of borohydride on the SERS of 4-NTA and 4-MTA is also examined to obtain further information on the relative ease of the sulfide to thiolate and nitro to amine conversions.

Parts a and b of Figure 5 show a series of SERS spectra taken for 4-NTA and 4-MTA, respectively, in Ag sols containing different amounts of excess  $\text{NaBH}_4$ ; all the spectra were obtained by flowing the sample solutions to minimize photoinduced spectral change. When the borohydride concentration is greater than 10 mM, the SERS spectrum of 4-NTA becomes identical not only to that of 4-MTA but also to that of 4-ABT. This implies that nitro to amine conversion as well as C–S bond scission takes place for 4-NTA on Ag in the presence of excess borohydride. When the borohydride concentration is near 5 mM, the SERS spectrum of 4-MTA can still be attributed to 4-ABT on Ag. However, the SERS spectrum of 4-NTA appears to be

a composite of 4-NBT and 4-ABT on Ag. In a separate work, the electrochemical potentials at an Ag wire electrode were measured to be  $-0.30$  and  $-0.50$  V vs SCE when  $\text{NaBH}_4$  was newly added to the Ag sol to obtain a final concentration of 5 and 10 mM, respectively (data not shown). This can also be understood by presuming that the C–S bond scission takes place prior to the nitro to amine conversion for 4-NTA on Ag. According to the cyclic voltammetry measurements, not only the sulfide to thiolate reduction but also the nitro to amine reduction persists until the electrode potential approaches the vicinity of  $-0.8$  V vs SCE. In the sol medium, however, features due to adsorbed sulfides can hardly be detected even when the sol potential is lowered at best to  $-0.3$  V. This is certainly due to the catalytic effect of Ag nanoparticles to relay electrons efficiently from borohydride to 4-NTA and 4-MTA.

In summary, we have investigated the adsorption and the visible-light-induced photoreaction characteristics of 4-NTA in Ag sol by SERS. The molecule itself is concluded to adsorb on Ag as 4-NTA via the sulfur atom. Upon irradiation by an argon ion laser at 514.5 nm, 4-NTA on Ag is found to convert to 4-ABT following two photoreactions, namely C–S bond scission followed by nitro to amine conversion. According to a separate CV study, electrochemically the C–S bond scission takes place at  $\sim -0.3$  V, while the nitro to amine conversion occurs at  $\sim -0.5$  V vs SCE. Much the same observation can be made by SERS after the addition of excess  $\text{NaBH}_4$  to Ag sols containing 4-NTA. All of these data suggest that the C–S bond scission occurs prior to the nitro to amine conversion even when 4-NTA on Ag is irradiated with 514.5 nm radiation. The present surface-induced photoreaction surely reflects one of the characteristics of silver nanoparticles functioning as moderate photoelectron emitters.

**Acknowledgment.** This work was supported by the Korea Research Foundation (KRF, 2003-015-C00285).

## References and Notes

- (1) Chang, R. K.; Furtak, T. E. *Surface Enhanced Raman Scattering*; Plenum Press: New York, 1982.
- (2) Moskovits, M. *Rev. Mod. Phys.* **1985**, *57*, 783.
- (3) Campion, A.; Kambhampati, P. *Chem. Soc. Rev.* **1998**, *27*, 241.
- (4) Kneipp, K.; Kneipp, H.; Itzkan, I.; Dasari, R. R.; Feld, M. S. *J. Phys.: Condens. Matter* **2002**, *14*, R597.
- (5) Moskovits, M. *J. Chem. Phys.* **1982**, *77*, 4408.
- (6) Schatz, G. C. *Acc. Chem. Res.* **1984**, *17*, 370.
- (7) Moskovits, M. *Rev. Mod. Phys.* **1985**, *57*, 783.
- (8) Schatz, G. C.; Van Duyne, R. P. In *Handbook of Vibrational Spectroscopy*; Griffiths, P. R., Ed.; Wiley: New York, 2001; p 1.
- (9) Moskovits, M.; Tay, L. L.; Yang, J.; Haslett, T. *Top. Appl. Phys.* **2002**, *82*, 215.
- (10) Otto, A. In *Light Scattering in Solid*; Cardona, M., Guntherodt, G., Eds.; Springer-Verlag: Berlin, 1984; Vol. IV, p 289.
- (11) Otto, A.; Mrozek, I.; Grabhorn, H.; Akemann, W. *J. Phys.: Condens. Matter* **1992**, *4*, 1143.
- (12) Otto, A. *Phys. Status Solidi A* **2001**, *188*, 1455.
- (13) Nitzan, A.; Brus, L. E. *J. Chem. Phys.* **1981**, *75*, 2205.
- (14) Goncher, G. M.; Harris, C. B. *J. Chem. Phys.* **1982**, *77*, 3767.
- (15) Goncher, G. M.; Parsons, C. A.; Harris, C. B. *J. Phys. Chem.* **1984**, *88*, 4200.
- (16) Wolkow, R. A.; Moskovits, M. *J. Chem. Phys.* **1987**, *87*, 5858.
- (17) Feilchenfeld, H.; Chumanov, G.; Cotton, T. M. *J. Phys. Chem.* **1996**, *100*, 4937.
- (18) Franzke, D.; Wokaun, A. *J. Phys. Chem.* **1992**, *96*, 6377.
- (19) Bjerneld, E. J.; Svedberg, F.; Johansson, P.; Käll, M. *J. Phys. Chem. A* **2004**, *108*, 4187.
- (20) Suh, J. S.; Moskovits, M.; Shakhsempour, J. *J. Phys. Chem.* **1993**, *97*, 1678.
- (21) Suh, J. S.; Jang, N. H.; Jeong, D. H.; Moskovits, M. *J. Phys. Chem.* **1996**, *100*, 805.
- (22) Jang, N. H.; Suh, J. S.; Moskovits, M. *J. Phys. Chem. B* **1997**, *101*, 8279.

- (23) Jeong, D. H.; Jang, N. H.; Suh, J. S.; Moskovits, M. *J. Phys. Chem. B* **2000**, *104*, 3594.
- (24) Jeong, D. H.; Suh, J. S.; Moskovits, M. *J. Phys. Chem. B* **2000**, *104*, 7462.
- (25) Jeong, D. H.; Suh, J. S.; Moskovits, M. *J. Raman Spectrosc.* **2001**, *32*, 1026.
- (26) Joo, T. H.; Yim, Y. H.; Kim, K.; Kim, M. S. *J. Phys. Chem.* **1989**, *93*, 1422.
- (27) Yim, Y. H.; Kim, K.; Kim, M. S. *J. Phys. Chem.* **1990**, *94*, 2552.
- (28) Lee, S. B.; Kim, K.; Kim, M. S. *J. Phys. Chem.* **1992**, *96*, 9940.
- (29) Lee, I.; Han, S. W.; Kim, C. H.; Kim, T. G.; Joo, S. W.; Jang, D.-J.; Kim, K. *Langmuir* **2000**, *16*, 9963.
- (30) Kim, K. L.; Lee, S. J.; Kim, K. *J. Phys. Chem. B*, in press.
- (31) Joo, T. H.; Kim, K.; Kim, M. S. *J. Mol. Struct.* **1987**, *162*, 191.
- (32) Joo, S. W.; Han, S. W.; Kim, K. *Appl. Spectrosc.* **2000**, *54*, 378.
- (33) Sun, S.; Birke, R. L.; Lombardi, J. R.; Leung, K. P.; Genack, A. Z. *J. Phys. Chem.* **1988**, *92*, 5965.
- (34) Han, S. W.; Lee, I.; Kim, K. *Langmuir* **2002**, *18*, 182.
- (35) Kim, K.; Lee, I.; Lee, S. J. *Chem. Phys. Lett.* **2003**, *377*, 201.
- (36) Lee, S. J.; Kim, K. *Chem. Phys. Lett.* **2003**, *378*, 122.
- (37) Han, H. S.; Han, S. W.; Kim, C. H.; Kim, K. *Langmuir* **2000**, *16*, 1149.
- (38) Ag sol was enforced to flow through a glass capillary (inner diameter: 1.1 mm) at a rate of 0.00153–0.06 mL·s<sup>-1</sup> using a syringe pump. Letting the flow rate of the sol be  $V_s$  (mL·s<sup>-1</sup>) and the cross-sectional area of the capillary be  $A_c$  (m<sup>2</sup>), the linear displacement rate of Ag colloidal particles through the capillary,  $u_{Ag}$  (m·s<sup>-1</sup>), can be denoted as  $u_{Ag} = 10^{-6} \cdot (V_s/A_c)$ . To estimate the laser dose quantitatively, it is then necessary to convolute  $u_{Ag}$  with the shape of the laser light. However, the distance to travel across the laser spot by Ag nanoparticles can be approximated to be  $\pi/4$  times the beam diameter ( $d_l$ ) of the laser at the sampling position, that is,  $d_l = 2 \mu\text{m}$ . The laser exposure time ( $t_{\text{exposure}}$ ) is then given by  $t_{\text{exposure}} = (\pi/4)(d_l/u_{Ag})$ ; thereby, for  $V_s = 0.06 \text{ mL}\cdot\text{s}^{-1}$ , for example, it becomes 0.025 ms.
- (39) Kim, K.; Kim, H. S.; Lee, S. J. *Langmuir* **2003**, *19*, 10985.
- (40) Jana, N. R.; Sau, T. K.; Pal, T. *J. Phys. Chem. B* **1999**, *103*, 115.